A first principles study of fluorescence quenching in rhodamine B dimers: how can quenching occur in dimeric species?†

Dani Setiawan,[ab] Andranik Kazaryan,[a] Muhamad Abdulkadir Martoprawiro[b] and Michael Filatov*[a]

Received 22nd March 2010, Accepted 25th May 2010
DOI: 10.1039/c004573j

Rhodamine B (RhB) is widely used in chemistry and biology due to its high fluorescence quantum yield. In high concentrations, the quantum yield of fluorescence decreases considerably which is attributed to the formation of RhB dimers. In the present work, a possible mechanism of fluorescence quenching in RhB dimers is investigated with the use of time-dependent density functional theory (TD-DFT). The excited states of monomeric and dimeric RhB species have been studied both in the gas phase and in solution with the use of the TD-BLYP/6-311G* method. Results of the calculations suggest that quenching can occur *via* an internal conversion to the charge-transfer singlet excited states, which can be followed by an intersystem crossing with the charge-transfer triplet states. A possibility to reduce the loss of the fluorescence quantum yield is discussed.

1. Introduction

Rhodamine B (RhB) is a chromophore from a family of xanthene dyes that is commonly used as an active medium in tunable lasers[1–3] due to its high fluorescence quantum yield (ϕ). It also finds a wide range of applications in materials science, chemistry and biology as a sensitizer in solar cells,[4] as a molecular probe,[5] as an electrochemical luminescence sensitizer,[6] as a water-tracing agent,[7] as a biological stain,[8] *etc*. High fluorescence quantum yield (>0.5) is observed in solution of RhB at low concentrations (10^{-4} to 10^{-6} M),[9–14] whereas at higher concentrations ($>10^{-3}$ M), the quantum yield decreases rapidly to less than 0.1.[9,15]

Currently, it is widely accepted that the quenching occurs *via* internal conversion and intersystem crossing in the excited states of aggregates (*e.g.*, dimers) of dyes in solution.[11,16–18] Indeed, xanthene dyes can form aggregates in polar solution due to the strong electrostatic and dispersion interactions between the dye molecules. For instance, RhB forms dimers in aqueous solution with an equilibrium constant of 2100 M^{-1}, at 20 °C.[19] Therefore, the fluorescence quantum yield of aqueous RhB can be strongly affected by dimerization, because dimers of RhB in water can only make a weak contribution to fluorescence, whereas they are capable of strong optical absorption.[20] It was suggested[21–23] that the intersystem crossing between the singlet and the triplet excited states can take place in RhB dimeric species thus leading to a radiationless decay channel that can not be realised in the monomeric species.

Because this mechanism is widely accepted, a large number of experimental works dealing with the synthesis of novel dye lasing materials attempt to avoid or decrease the possibility of dimer formation.[8,11,24–30] It was assumed that larger concentrations of dyes and reduced aggregate formation could be achieved *via* incorporating dyes into solid matrices or attaching them to polymer chains. However, many of these works ended up with lower quantum yields as compared to aqueous dyes.[24–28]

Therefore, it is desirable to investigate the fluorescence quenching mechanism and to analyze whether the intersystem crossing can be responsible for the low quantum yield in dimeric species. Direct experimental evidence of the fluorescence quenching *via* intersystem crossing in dimers is rather difficult to obtain. Furthermore, we are not aware of experimental or systematic *ab initio* theoretical studies which attempted to establish the relative ordering of the singlet and triplet excited states in RhB dimers. Thus, the purpose of this work is to fill this gap.

In this article, we undertake a time-dependent density functional theory(TD-DFT) study of the ground and the lowest singlet and triplet excited states of monomeric cationic RhB and of various conformations of dimeric $(RhB)_2^{2+}$ species. The primary purpose of this study is to investigate the feasibility of the fluorescence quenching *via* the intersystem crossing mechanism and to analyze possible ways of reducing the quenching. Special attention is paid to the charge-transfer excitations in RhB dimeric species, which will be shown to play an important role in the fluorescence quenching. The relative role of intra-molecular and charge-transfer excitations in dimeric species is analyzed with the help of a simple analytic model derived in this work. Theoretical methods and models used in the present work are described in section 2. The computational results for monomeric and dimeric RhB species are presented and analyzed in section 3 and a possibility to reduce the fluorescence quenching is discussed.

[a] *Theoretical Chemistry, Zernike Institute for Advanced Materials, Rijksuniversiteit Groningen, Nijenborgh 4, Groningen 9747AG, The Netherlands. E-mail: m.filatov@rug.nl*
[b] *Department of Chemistry, Institut Teknologi Bandung, Jalan Ganesha 10, Bandung 40132, Indonesia*

† Electronic supplementary information (ESI) available: Model details. See DOI: 10.1039/c004573j

2. Models and method of calculation

In the liquid phase, RhB can exist in three conformations: cationic, lactonic, and zwitter-ionic as shown in Fig. 1. While cationic and zwitter-ionic conformations exist in polar solvents, cationic in acidic and zwitter-ionic in basic solution, lactonic is only found in non-polar or polar aprotic solvents.[31] It is also observed that the cationic and zwitter-ionic conformations fluoresce, but not the lactonic. In solution, there exists an equilibrium between different forms of RhB.[32–35] However, in this work, we will focus on the cationic form, the most common conformation when RhB is anchored on the polymeric substrate, because attachment of RhB dyes to polymer chains is usually done *via* their carboxyl group.[27,36,37]

The dimeric species considered in the present work are shown in Fig. 2. Full geometry optimization was carried out for monomeric RhB and partial geometry optimization was carried out for dimeric species: the intermolecular distance was optimized while keeping all other geometric parameters fixed at their values in the monomeric species (see section 3.2). In these calculations, the solvent effects are included *via* a conductor-like polarizable continuum model (CPCM).[38] The counter ions, Cl^-, are not taken into account.

The singlet and triplet excited states of the dimeric species are calculated with the use of TD-DFT. To simplify the identification of the excited states in dimeric RhB species, we used a simple four-electron–four-orbital model, eqn (1), described in more detail in the ESI†. This model takes into account only frontier molecular orbitals (MOs) of dimers which are formed as the in-phase and out-of-phase linear combinations of the HOMOs and LUMOs of the monomers. This results in four frontier orbitals of the dimer upon aggregation (Fig. 3). The many-electron states of dimer are constructed as the linear combinations of the Slater determinants corresponding to different populations of the four frontier orbitals.

The lowest excited states are the spin-adapted linear combinations of the singly excited determinants (see ESI†): four singlet excited states and four triplet excited states of the dimer. These excited states can be classified as: two intramolecular (local) singlet excitations (IE-S), two charge-transfer singlet excited states (CT-S), two intramolecular triplet excitations (IE-T), and two charge-transfer triplet states (CT-T) (Fig. 4). The CT-S and CT-T states are degenerate within this model, which simplifies the identification of the respective states in the TD-DFT calculations.

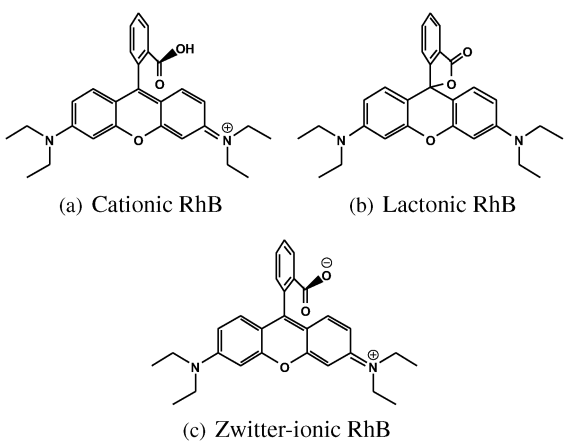

(a) Cationic RhB (b) Lactonic RhB

(c) Zwitter-ionic RhB

Fig. 1 RhB in cationic (a), lactonic (b), and zwitter-ionic (c) conformations.

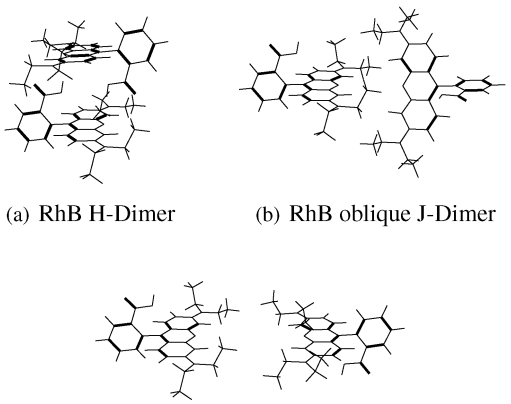

(a) RhB H-Dimer (b) RhB oblique J-Dimer

(c) RhB tilted J-Dimer

Fig. 2 Geometries of RhB dimers.

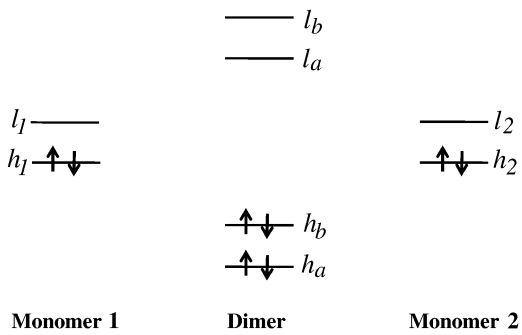

Fig. 3 Frontier orbitals of dimer and of monomeric units used in a simple 4 electron–4 orbital model.

$$E^S_{3,4} \approx \varepsilon_0 + K_1 \pm \tfrac{3}{2}K_2 \quad (1)$$

$$E^S_{1,2} \approx \varepsilon_0 \pm \tfrac{1}{2}K_2$$

$$E^T_{3,4} \approx \varepsilon_0 \pm \tfrac{1}{2}K_2$$

$$E^T_{1,2} \approx \varepsilon_0 - K_1 \pm \tfrac{1}{2}K_2$$

In eqn (1), ε_0 is the HOMO–LUMO gap of the monomer and $K^1 = (h_1l_1|h_1l_1)$, $K_2 = (h_1l_1|h_2l_2)$ are the exchange integrals between the respective HOMOs and LUMOs of the monomeric units. Depending on the parameters of the model, the CT states may be found within the same energy interval as the intramolecular excitations. Because the energies of charge-transfer excitations in TD-DFT suffer from the self-interaction error (SIE), which may lead to an artificial stabilization of these states with respect to the intramolecular excitations, an *a posteriori* asymptotic correction from the ΔSCF calculation[39,40] was applied to the excitation energies of the charge-transfer states of dimers.

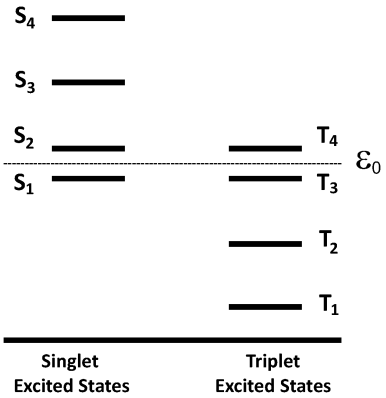

Fig. 4 Ordering of the lowest excited states of the dimer as obtained from the 4 electron–4 orbital model.

3. Results and discussion

In this section, we analyze the excited states of the monomer cationic RhB and dimeric RhB species with the use of density functional calculations. Several density functionals are applied to optimize the molecular geometry of these species and to calculate their electronic excitation energies. Based on these calculations, a functional that yields the excitation energies in the best agreement with the experiment is selected. With the use of this functional, the relative ordering of the intramolecular and charge transfer (CT) excited states of the RhB dimeric species as a function of the mutual orientation of the monomeric units and the distance between them is investigated. Implications for the fluorescence quenching are also analyzed.

3.1 Excited states of RhB monomeric species

Calculations of the monomeric cationic RhB species are carried out with the use of the BLYP,[41,42] B3LYP,[43,44] and BH&HLYP[45]density functionals and the 6-311G* basis set. Geometry optimization in the gas phase and in aqueous solution have been carried out with the use of the respective density functional and the lowest singlet and triplet excitation energies were obtained in the TD-DFT calculations using the optimized geometries. The obtained excitation energies are compared in Table 1 with the available experimental data. This comparison shows that the BLYP density functional yields the excitation energy of the cationic RhB in water in the closest agreement with the experiment (see Table 1).

TD-BLYP/6-311G* predicted two absorption peaks for monomeric cationic RhB^+ in water: at 528.18 nm ($S_0 \rightarrow S_1$ transition with the oscillator strength $f = 0.85$) and at 404.61 nm ($S_0 \rightarrow S_4$ with $f = 0.13$). The latter, which is somewhat underestimated by TD-BLYP, corresponds to the RhB^+ experimental absorption peak in the UV region (*ca.* 360 nm).[47] The lowest S_1 singlet excited state corresponds to the excitation of a single electron from the highest occupied molecular orbital (HOMO) to the lowest unoccupied molecular orbital (LUMO).

Table 1 Lowest excitation energy of the cationic RhB as obtained in the TD-DFT calculations with the 6-311G* basis set. Experimental data taken from Arbeloa *et al.*[46]

	Gas phase/nm	Water/nm
Experimental	N/A	557.0
BLYP	511.61	528.18
B3LYP	462.72	481.97
BH&HLYP	414.97	431.80
HF	361.41	373.43

The lowest T_1 triplet excited state corresponds to the HOMO–LUMO transition and lies 0.79 eV below the S_1 state (Fig. 5). This makes the singlet–triplet interconversion quite improbable, because due to a very weak spin–orbit coupling the intersystem crossing in organic molecular systems can occur only *via* surface crossing points. Given such an energy difference it is not expected that the surface crossing may occur sufficiently close to the Franck–Condon point. Thus, these observations are consistent with the experimental result, that there is a high quantum yield of fluorescence in the monomeric form of RhB.

3.2 Excited states of RhB dimeric species

To achieve a qualitative understanding of the optical properties of dimeric RhB species a partial geometry optimization was deemed sufficient. During the partial geometry optimization, the geometries of the monomeric units were kept fixed and only the distance between these units and the angle between the molecular planes of the monomers were optimized. The BLYP density functional and the 6-311G* basis set were used in the optimization. The calculations were carried out in aqueous solution using the CPCM solvation method. Because the Cl^- counter-ions were not included in our calculations, only local minima on the otherwise repulsive potential energy curves of the $(RhB)_2^{2+}$ species were obtained. Local energy minima are found at a distance of 3.655 Å for the oblique J-dimer and at 6.129 Å for the H-dimer, while no local minimum was found for the tilted J-dimer configuration.

For comparison, the H-dimer geometry was fully optimized with the BLYP/6-311G* method in aqueous solution. The root mean square deviation (RMSD) of the atomic coordinates in the fully optimized and in the partially optimized dimer geometries amounts to 0.485 Å (0.243 Å per monomer unit). Given the small RMSD value it is not expected that the use of fully optimized geometries may lead to noticeable differences in the calculated excitation spectra. Furthermore, the full geometry optimization could not be finished for all the dimeric species due to certain technical difficulties experienced in the CPCM calculations. Therefore, for the sake of consistency, the

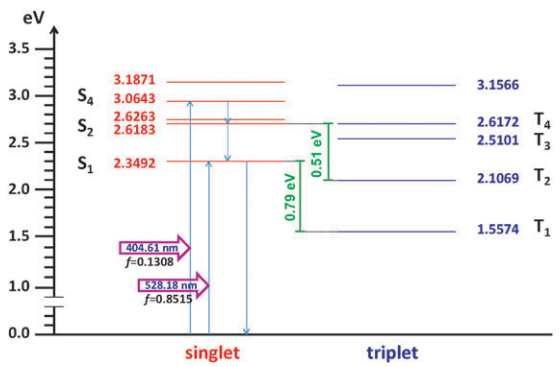

Fig. 5 Lowest singlet and triplet excited states of RhB^+.

partially optimized geometries of the dimeric species were used throughout this work.

Using these geometries, the excitation energies of the H-dimer and the oblique J-dimer were calculated with the three density functionals, BLYP, B3LYP, and BH&HLYP. In the $(RhB)_2^{2+}$ species, the most important low-lying electronic excitations are the superpositions of the transitions between the frontier orbitals of the dimer: (HOMO − 1) → (LUMO), (HOMO − 1) → (LUMO + 1), (HOMO) → (LUMO), and (HOMO) → (LUMO + 1). As discussed in section 2, the frontier orbitals of $(RhB)_2^{2+}$ are the superpositions of the HOMO and the LUMO of the two monomers. Analysis of the excitation amplitudes and orbital transitions obtained from the TD-DFT calculations shows that the S_1 and S_2 singlet excited states and the T_3 and T_4 triplet excited states have intermolecular charge-transfer character. As shown in Fig. 6, the pairs of states S_1–T_3 and S_2–T_4 are degenerate. This is in accord with the 4-electron–4-orbital model which predicts occurrence of the degenerate pairs of singlet and triplet states with charge-transfer character. The S_3 and S_6 singlet excited states and the T_1 and T_2 triplet excited states of the dimer are the superpositions of the intramolecular excitations of the two monomers. The dipole allowed transition $S_0 \rightarrow S_6$ has the oscillator strength $f = 1.62$ whereas transitions to the other states have vanishingly small (S_3) or zero (S_1 and S_2) oscillator strengths. Thus the absorption spectrum of the dimeric $(RhB)_2^{2+}$ species is dominated by the $S_0 \rightarrow S_6$ excitation. In Table 2, the $S_0 \rightarrow S_6$ excitation energies obtained from the TD-DFT calculations with the three density functionals are compared with the experimentally observed maximum of the absorption spectrum. Similar to the monomeric cationic RhB species, the BLYP density functional yields the excitation energies in the best agreement with the experiment. Therefore, the further analysis of the fluorescence quenching is based on the TD-BLYP/6-311G* results.

The charge-transfer singlet and triplet excited states of the dimeric $(RhB)_2^{2+}$ species are affected by the electron self-interaction error inherent in approximate density functionals. The SIE results in an artificial lowering of the excitation energy of these states as compared to the intra-molecular excitations. The magnitude of the lowering can be evaluated with the use of the ΔSCF approach (which is self-interaction free)

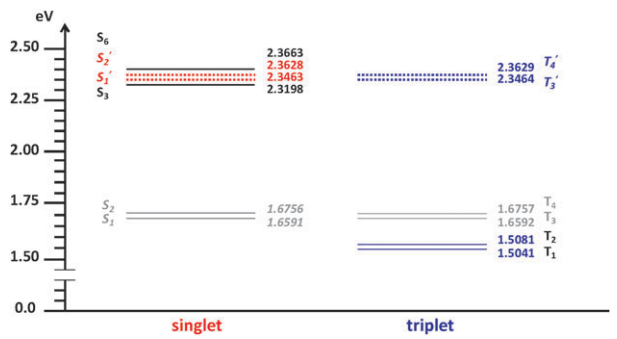

Fig. 6 Lowest excited states of H-type $(RhB)_2^{2+}$, calculated with 6-311G* basis set in water. The S_1', S_2', T_3', and T_4' energy levels (dashed lines) of the charge-transfer excited states are corrected for the self-interaction error of the approximate density functional as given in eqn (3). The uncorrected energy levels are shown with shadowed lines.

Table 2 Lowest optical excitation energies of $(RhB)_2^{2+}$ species (in aqueous solution) as obtained in TD-DFT calculations with the 6-311G* basis set. Experimental data are taken from (a), Alig *et al.*,[32] (b) Bojarski *et al.*,[48] and (c) Kemnitz *et al.*[49]

		J-Dimer (Oblique)/nm	
	H-Dimer/nm	Peak I	Peak II
Experimental	525.0[a]–530.0[b]	Broad peak between 570 and 590[c]	
BLYP	522.5	524.0	533.3
B3LYP	476.3	476.7	485.6
BH&HLYP	427.5	429.3	436.2
HF	237.5	371.3	376.8

whereby the CT excitation energy for a dimer at large intermonomer separation is evaluated as a sum of the ionization potential of the donor (D) unit and the electron affinity of the acceptor (A) unit.

$$E_{CT}^{\Delta SCF} = IP_{(D)} - EA_{(A)} = (E_{(D^+)} + E_{(A^-)}) - (E_{(D^0)} + E_{(A^0)}) \quad (2)$$

At large intermonomer separation in the $(RhB)_2^{2+}$ dimer, transfer of one electron between the monomer units results in the $(RhB)^0$–$(RhB)^{2+}$ configuration. Therefore, in the CT excited state, there is no long-range electrostatic interaction between the donor and acceptor units. Hence, the difference between the CT excitation energy obtained in a TD-DFT calculation at large intermonomer separation and the ΔSCF energy (eqn (2)) can be used as a correction to the CT excitation energies obtained in TD-DFT calculations at shorter intermonomer separations R. We believe that with the use of the corrected CT excitation energies,

$$E_{corr\text{-}CT}^{TD\text{-}DFT}(R) = E_{CT}^{TD\text{-}DFT}(R) + (E_{CT}^{\Delta SCF} - E_{CT}^{TD\text{-}DFT}(\infty)), \quad (3)$$

the bulk of the SIE in the TD-DFT CT excitation energies of the $(RhB)_2^{2+}$ dimer is compensated.

To obtain the corrected TD-DFT CT excitation energies, $E_{corr\text{-}CT}^{TD\text{-}DFT}$, the TD-BLYP/6-311G* excitation energies of $(RhB)_2^{2+}$ were calculated at various intermonomer separations. Because beyond $R = 10$ Å the CT singlet and triplet excitation energies remain constant, the $E_{CT}^{TD\text{-}DFT}$ at $R = 40$ Å was taken as a reference value $E_{CT}^{TD\text{-}DFT}(\infty)$ for use in eqn (3). From eqn (3), a correction of 0.687 eV was obtained for the TD-DFT CT excitation energies. The corrected CT singlet and triplet excitation energies of the $(RhB)_2^{2+}$ dimer are reported in Table 3 along with the intramolecular excitation energies.

At the equilibrium intermonomer separation in the H-dimer (see Fig. 6), the corrected CT singlet excitation energies occur between the intramolecular excitation energies. It is noteworthy that the two CT singlet excited states fall below the optically accessible S_6 state. Of note, in a recent theoretical study, Pabst and Köhn[50] found that the charge-transfer excited states may occur below the intramolecular excited states in π-stacked systems. It can therefore be conjectured that, in H-dimers, an internal conversion of the excitation from the optically accessible singlet excited state to the CT singlet excited states may take place. This conjecture is indirectly confirmed by the experimental observation by Wasielewski and co-workers[51,52] of the fluorescence quenching due to

Table 3 Dependence of the TD-BLYP/6-311G* excitation energies of the $(RhB)_2^{2+}$ H-dimer on the intermonomer distance. The CT excitation energies are corrected for the SIE using eqn (3). The oscillator strength values are given in parentheses

	Singlet states energy/eV				Triplet states energy/eV	
Interplanar distance/Å	S_6	S_3	S_2	S_1	T_4	T_3
6	2.366 (1.703)	2.320 (0.001)	2.363 (0.000)	2.346 (0.000)	2.363 (0.000)	2.346 (0.000)
10	2.342 (1.693)	2.308 (0.0002)	2.383 (0.000)	2.382 (0.000)	2.383 (0.000)	2.382 (0.000)
15	2.337 (1.718)	2.324 (0.0002)	2.383 (0.000)	2.383 (0.000)	2.383 (0.000)	2.383 (0.000)
20	2.332 (1.715)	2.325 (0.0002)	2.383 (0.000)	2.383 (0.000)	2.383 (0.000)	2.383 (0.000)
40	2.327 (1.725)	2.326 (0.009)	2.383 (0.000)	2.383 (0.000)	2.383 (0.000)	2.383 (0.000)

spontaneous charge separation resulting from interaction with the solvent and fluctuations of the molecular geometry. It was also found experimentally by Loutfy and Sharp[53] that, in xanthene dyes, the fluorescence quenching may occur as a result of a bimolecular photoredox reaction that involves intermolecular electron transfer in the excited states.

The suggested internal conversion should result in a considerable decrease of the fluorescence quantum yield, because a large fraction of the excited state population is transferred to optically dark (CT) states. Furthermore, because the CT triplet excited states are (nearly) degenerate with the CT singlet excited states, there are favourable conditions for the intersystem crossing which can lead to the formation of long-living triplet excited states. Thus, the results of the TD-DFT calculations on H-dimers help to understand the experimental observations of fluorescence quenching in H-dimers.[9,15]

For the cationic oblique RhB J-dimer, the TD-BLYP/6-311G* calculations yield two major absorption peaks: at 524.0 nm with the oscillator strength $f = 1.05$ and at 533.3 nm with $f = 0.56$. The first peak corresponds to the $S_0 \rightarrow S_3$ excitation and the second to the $S_0 \rightarrow S_6$ excitation (see Fig. 7). Thus, both intramolecular excited states of the RhB J-dimer are populated *via* the optical excitation. It is noteworthy though that the CT singlet excited states (corrected for the SIE as described above) lie above the intramolecular excited states. Although the energy gap is rather narrow, *ca.* 0.05 eV (430 cm^{-1}), it may result in a considerably reduced probability of population of the CT states *via* the thermal excitation ($kT \approx 360$ cm^{-1} at 300 K). Thus, there should be almost no quenching of fluorescence in the RhB J-dimers due to internal conversion to the CT excited states. This result is consistent with the experimental observation of fluorescence from the $(RhB)_2^{2+}$ J-type dimers, which is more intense than from the H-dimers and occurs in the range between 570 nm and 590 nm.[49]

It is interesting to note that the population of the intramolecular excited states depends on the mutual orientation of the monomer units in the dimer. Thus, in the $(RhB)_2^{2+}$ H-dimer, the upper, S_6, state is predominantly populated *via* the optical excitation, whereas in the J-dimer both states, S_3 and S_6, are populated. If it were possible to populate only the lower state *via* the optical excitation, it would help to enhance the fluorescence from this state, because quenching due to the internal conversion to the CT states would become less significant. The dependence of fluorescence on the mutual orientation of the monomer units in aggregates of chromophores has been studied by McRae and Kasha[54] with the use of the point dipole approximation. Although this approximation is valid only at large intermolecular separations, our TD-DFT calculations on RhB dimers yield results which are consistent with the McRae–Kasha model.

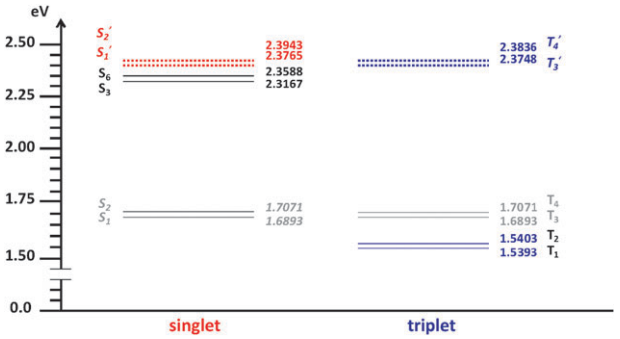

Fig. 7 Lowest excited states of J-type $(RhB)_2^{2+}$, calculated with 6-311G* basis set in water. The S_1', S_2', T_3', and T_4' energy levels (dashed lines) of the charge transfer excited states are corrected for the self-interaction error of the approximate density functional as given in eqn (3). The uncorrected energy levels are shown with shadowed lines.

To study the orientational dependence of the low lying excitations of the $(RhB)_2^{2+}$ dimers, we carried out TD-BLYP/6-311G* calculations on the dimers with varying dihedral angle between the planes of the monomer units. In these calculations, a number of dimeric structures were generated varying between a co-facial arrangement of the monomer units (as in the H-type dimer) and a co-planar arrangement with both monomers lying in the same plane. Table 4 shows the results of the TD-DFT calculations for the low lying excitation energies as a function on the interplanar dihedral angle α (Fig. 8).

In a co-facial dimer with a collateral orientation of the intramolecular transition dipole moments the optical excitation occurs predominantly to the upper, S_6, intramolecular excited state, whereas, in a co-planar dimer with collinear orientation of the transition dipole moments of the monomers, it is the lower, S_3, state that is populated *via* the optical excitation

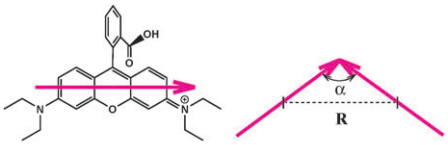

(a) (b)

Fig. 8 (a) Dipole moment of the lowest optically allowed transition of RhB^+ and (b) angle between transition dipole moments of $(RhB)_2^{2+}$.

Table 4 Lowest excited states of $(RhB)_2^{2+}$ as a function of interplanar dihedral angle α as obtained from the TD-BLYP/6-311G* calculations. The charge-transfer excited states were corrected for the self-interaction error (see text). The oscillator strengths of the transitions are given in parentheses

	Singlet states energy/eV				Triplet states energy/eV	
α	S_6	S_3	S_2	S_1	T_4	T_3
2.4°	2.3624 (1.6970)	2.3080 (0.0025)	2.3888 (0.0000)	2.3879 (0.0000)	2.3888 (0.0000)	2.3879 (0.0000)
88.5°	2.3368 (0.8788)	2.3194 (0.8666)	2.3871 (0.0000)	2.3859 (0.0000)	2.3871 (0.0000)	2.3859 (0.0000)
106.5°	2.3341 (0.6009)	2.3189 (1.1650)	2.3875 (0.0000)	2.3846 (0.0000)	2.3875 (0.0000)	2.3846 (0.0000)
168.1°	2.3484 (0.0201)	2.3162 (1.8303)	2.3865 (0.0000)	2.3864 (0.0000)	2.3865 (0.0000)	2.3864 (0.0000)

(Table 4). At the intermediate dihedral angles, both states, S_3 and S_6, have non-zero oscillator strength which become (nearly) equal at the angle of 88.5°. These results are consistent with the McRae–Kasha model which predicts that, at a collateral orientation of the transition dipole moments of the monomer units, the optical transition occurs to the upper state (S_6, in our case), at a collinear orientation, the transition occurs to the lower state and, at an angle α of *ca.* 80.6°, both intramolecular excited states of the dimer are equally populated.

From the described dependence of the oscillator strength on the mutual orientation of the monomer units in the dimer, it can be concluded that the geometric conformations in which the transition dipole moments of the monomers are (nearly) collinear should be beneficial for the fluorescence quantum yield. Indeed, in these conformations, the lowest of the intramolecular excited states of the dimer is predominantly populated *via* the optical excitation. Because this state is below the CT excited states and the other intramolecular excited state, the probability of internal conversion to any of these states is rather low and the quantum yield of fluorescence is expected to be large.

4. Conclusions

The low lying excited states of the cationic rhodamine B, RhB^+, and various conformations of the cationic $(RhB)_2^{2+}$ dimer were studied with the use of TD-DFT calculations employing the BLYP density functional and the 6-311G* basis set. The excitation energies obtained in the TD-BLYP/6-311G* calculations are in a good agreement with the experimentally observed absorption spectra of the monomeric and dimeric RhB species. On the basis of our calculations, the observed quenching of fluorescence in RhB dimers can be explained due to internal conversion of the optically bright intramolecular excited state to the (optically dark) states with the intermolecular charge-transfer character. This conclusion is supported by the experimental observation of the fluorescence quenching in dimers of perylene-based chromophores which occurs *via* spontaneous charge separation in the excited state.[51,52] Therefore, the suggested fluorescence quenching mechanism may have rather general character and may occur in various fluorescent systems, such as xanthene dyes, organometallic-based sensitizers for solar cells,[55,56] *etc.*

The TD-DFT calculations predict that the CT excited states of the $(RhB)_2^{2+}$ dimers occur in the same narrow energy range as the (optically active) intramolecular excited states. This creates a possibility for the internal conversion to the CT excited states and results in a considerable reduction of the fluorescence quantum yield. However, ordering of the excited states of RhB dimers depends on the mutual orientation of the monomer units. Thus, in the H-dimer arrangement, the strongly absorbing intramolecular excited state lies above the CT excited states, whereas in the J-type dimers a reversed ordering of the excited states is observed. It can therefore be suggested that, for obtaining a higher fluorescence quantum yield, *e.g.* in solid-state dye laser applications, the conformations of dimers in which the monomer units have (nearly) collateral arrangement of the transition dipole moments should be avoided. It is expected that, in synthetic systems with the dye molecules incorporated into a solid-state matrix or anchored on a surface, the greatest fluorescence quantum yield can be acheived if the arrangement of dye molecules is reminiscent of the J-type dimers with the angle between transition dipole moments varying in the range $80° < \alpha < 180°$.

References

1 D. L. Andrews, *Lasers in Chemistry*, Springer-Verlag, Berlin, 1997.
2 F. P. Schafer, *Dye Lasers*, Springer-Verlag, Berlin, 2nd edn, 1977, p. 1.
3 M. Maeda, *Laser Dyes: Properties of Organic Compounds of Laser Dyes*, Academic Press Inc., Orlando, 1984, p. 22.
4 M. Fujihara, M. Kubota and T. Osa, *J. Electroanal. Chem.*, 1981, **119**, 379.
5 E. Kato and T. Murakami, *Polym. Gels Networks*, 1998, **6**, 179.
6 C. Zhang, G. Zhou, Z. Zhang and M. Aizawa, *Anal. Chim. Acta*, 1999, **165**, 394.
7 S. P. Liu, Z. F. Liu and H. Q. Luo, *Anal. Chim. Acta*, 2000, **407**, 255.
8 R. K. Ward, P. N. Nation, M. Maxwell, C. L. Barker and R. H. Clothier, *Toxicol. in Vitro*, 1997, **11**, 633.
9 F. L. Arbeloa, P. R. Ojeda and I. L. Arbeloa, *J. Lumin.*, 1989, **44**, 105.
10 K. G. Casey and E. L. Quitevis, *J. Phys. Chem.*, 1988, **92**, 6590.
11 K. H. Drexhage, *Structure and Properties of Laser Dyes*, Springer-Verlag, Berlin, 2nd edn, 1977, p. 144.
12 R. E. Kellogg and R. G. Bennett, *J. Chem. Phys.*, 1964, **41**, 3042.
13 R. F. Kubin and A. N. Fletcher, *J. Lumin.*, 1983, **27**, 455.
14 M. J. Snare, F. E. Treloar, K. P. Ghiggino and P. J. Thistlethwaite, *J. Photochem.*, 1982, **18**, 335.
15 C. V. Bindhu and S. S. Harilal, *Anal. Sci.*, 2001, **17**, 141.
16 K. K. Rohatgi and G. S. Singhal, *J. Phys. Chem.*, 1966, **70**, 1695.
17 N. O. Mchedlov-Petrosyan and Y. V. Kholin, *Russ. J. Appl. Chem.*, 2004, **77**, 414.
18 O. Valdes-Aguilera and D. C. Neckers, *Acc. Chem. Res.*, 1989, **22**, 171.

19 I. L. Arbeloa and P. R. Ojeda, *Chem. Phys. Lett.*, 1981, **79**, 347.
20 J. Muto, *J. Phys. Chem.*, 1976, **80**, 1342.
21 R. W. Chambers, T. Kajiwara and D. R. Kearns, *J. Phys. Chem.*, 1974, **78**, 380.
22 J. M. Hernando, M. van der Schaaf, E. M. H. P. van Dijk, M. Sauer, M. F. G. Parajo and N. F. van Hulst, *J. Phys. Chem. A*, 2003, **43**, 107.
23 H. Schmidt, *J. Phys. Chem.*, 1976, **80**, 2959.
24 C. M. Carbonaro, A. Annedda, S. Grandi and A. Magistris, *J. Phys. Chem. B*, 2006, **110**, 12932.
25 A. Costela, I. Garcia-Moreno, C. Gomez, O. Garcia, R. Sastre, A. Roig and E. Molins, *J. Phys. Chem. B*, 2005, **109**, 4475.
26 A. C. I. Garcia-Moreno, A. Cuesta, O. Garcia, D. del Agua and R. Sastre, *J. Phys. Chem. B*, 2005, **109**, 21618.
27 D. Setiawan, D. Wahyuningrum, R. Hidayat, T. M. On and S. Achmad, in preparation.
28 S. Singh, V. R. Kanetkar, G. Sridhara, V. Muthuswamy and K. Rajab, *J. Lumin.*, 2003, **101**, 285.
29 W. J. Ward, J. R. Cramm, P. E. Reed and B. S. Johnson, *Derivatized Rhodamine Dye and Its Copolymers*, *US Pat*. No. 5 772 894, 1998.
30 W. J. Ward, J. R. Cramm, P. E. Reed and B. S. Johnson, *Derivatized Rhodamine Dye and Its Copolymers*, *US Pat*. No. 5 808 103, 1998.
31 J. Karpiuk, Z. R. Grabowski and F. C. D. Schryver, *J. Phys. Chem.*, 1994, **98**, 3247.
32 A. R. G. Alig, D. Gourdon and J. Israelachvili, *J. Phys. Chem. B*, 2007, **111**, 95.
33 D. A. Hinckley and P. G. Seybold, *Spectrochim. Acta*, 1988, **44A**, 1053.
34 R. W. Ramette and E. B. Sandell, *J. Am. Chem. Soc.*, 1956, **78**, 4872.
35 H. Watarai and F. Funaki, *Langmuir*, 1996, **12**, 6717.
36 A. Costela, I. Garcia-Moreno, J. M. Figuera, F. Amat-Guerri, R. Mallavia and R. Sastre, *J. Appl. Phys.*, 1996, **80**, 3167.
37 H. Tian, Y. He and C. P. Chang, *J. Mater. Chem.*, 2000, **10**, 2049.
38 V. Barone and M. Cossi, *J. Phys. Chem.*, 1998, **102**, 1995.
39 M. E. Casida and D. R. Salahub, *J. Chem. Phys.*, 2000, **113**, 8918.
40 A. Dreuw, J. L. Weisman and M. Head-Gordon, *J. Chem. Phys.*, 2003, **119**, 2943.
41 A. D. Becke, *Phys. Rev.*, 1988, **A38**, 3098.
42 C. Lee, W. Yang and R. G. Parr, *Phys. Rev.*, 1988, **B37**, 785.
43 P. J. Stephens, F. J. Devlin, C. F. Chabalowski and M. J. Frisch, *J. Phys. Chem.*, 1994, **98**, 11623.
44 R. H. Hertwig and W. Koch, *Chem. Phys. Lett.*, 1997, **268**, 345.
45 A. D. Becke, *J. Chem. Phys.*, 1993, **98**, 1372.
46 I. L. Arbeloa and K. K. Rohatgi Mukherjee, *Chem. Phys. Lett.*, 1986, **128**, 474.
47 H. Du, R. A. Fuh, J. Li, A. Corkan and J. S. Lindsey, *Photochem. Photobiol.*, 1998, **68**, 141.
48 P. Bojarski and A. Jankowics, *J. Lumin.*, 1999, **81**, 21.
49 K. Kemnitz, N. Tamai, I. Yamazaki, N. Nakashima and K. Yoshihara, *J. Phys. Chem.*, 1986, **90**, 5094.
50 M. Pabst and A. Köhn, *J. Phys. Chem. A*, 2010, **114**, 1639.
51 M. J. Fuller, A. V. Gusev and M. R. Wasielewski, *Isr. J. Chem.*, 2004, **44**, 101.
52 J. M. Giaimo, A. V. Gusev and M. R. Wasielewski, *J. Phys. Chem. B*, 2002, **124**, 8530.
53 R. O. Loutfy and J. H. Sharp, *Photogr. Sci. Eng.*, 1976, **20**, 165.
54 E. G. McRae and M. Kasha, *J. Chem. Phys.*, 1958, **28**, 721.
55 G. Benkö, J. Kallioinen, P. Myllyperkiö, F. Trif, J. Korppi-Tommola, A. P. Yartsev and V. Sundström, *J. Phys. Chem. B*, 2004, **108**, 2862.
56 P. Myllyperkiö, G. Benkö, J. Korppi-Tommola, A. P. Yartsev and V. Sundström, *Phys. Chem. Chem. Phys.*, 2008, **10**, 996.

